Electronic Notes in Theoretical Computer Science 66 No. 1 (2002)
URL: http://www.elsevier.nl/locate/entcs/volume66.html 13 pages

Computability of Partial Delaunay Triangulation and Voronoi Diagram

[Extended Abstract]

A. A. Khanban [a,1], A. Edalat [a,2] and A. Lieutier [b,3]

[a] *Department of Computing, Imperial College, London, U.K.*

[b] *Dassault Systemes Provence, Aix-en-Provence & LMC/IMAG, Grenoble, France*

Abstract

Using the domain-theoretic model for geometric computation, we define the partial Delaunay triangulation and the partial Voronoi diagram of N partial points in $\mathbb{R}^2$ and show that these operations are domain-theoretically computable and effectively computable with respect to Hausdorff distance and Lebesgue measure. These results are obtained by showing that the map which sends three partial points to the partial disc passing through them is computable. This framework supports the design of robust algorithms for computing the Delaunay triangulation and the Voronoi diagram with imprecise input.

1 Introduction

In [5], a new model for geometric computation was introduced which is based on domain theory and recursion theory, and supports a methodology for designing robust geometric algorithms in the context of exact real number inputs as well as in the framework of uncertain or imprecise input data. This model thus provides a new framework for computational geometry in which the input and output of geometric algorithms are partial objects.

In [6], this model was used to define the partial convex hull of N imprecise or partial points, i.e. rectangles, in $\mathbb{R}^n$ and to show that the convex hull of N computable points is indeed computable and that it can be approximated effectively by a sequence of rational (or dyadic) partial convex hulls which converge effectively to the convex hull both with respect to the Hausdorff

[1] Email: khanban@doc.ic.ac.uk
[2] Email: ae@doc.ic.ac.uk
[3] Email: andre_lieutier@ds-fr.com

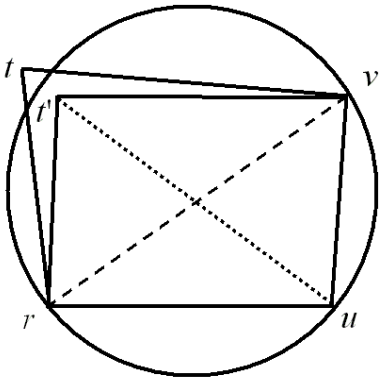

Fig. 1. Effect of imprecise input in Delaunay triangulation.

metric and the Lebesgue measure. Furthermore, an algorithm to compute the partial convex hull was presented, which is $N \log N$ in 2d and 3d.

In this paper, we aim to tackle the problem of computability of the partial Delaunay triangulation and the partial Voronoi diagram of a finite number of partial points, i.e. rectangles, in the plane. In fact, despite a great number of algorithms and articles published on robustness issues related to the Delaunay triangulation and the Voronoi diagram of a finite number of points in the plane [18], [8], [17], [14], [1], [2], [4], [9], [10], the question of computability of the Delaunay triangulation and the Voronoi diagram for imprecise input points have not been previously addressed. In [4], the naive interval calculation as in [13] has been compared with the results based on a new idea called "tangent circles", which is nearly 16 times better. In [12], we have even better results, in particular when the inputs are rectangles, as it is usually the case.

Robustness problems arise from the discrepancy between the unrealistic real RAM machine model [16], used to prove the correctness of algorithms, and real computers which are only able to deal with finite data. Mathematically correct algorithms in this model, when implemented in floating point arithmetic, become unreliable and lead to inconsistencies and potentially disastrous results. These inconsistencies are consequence of numerical errors in evaluating the predicates in the combinatorial, i.e. the symbolic, logical or topological, part of geometric algorithms. The problem is related to the fact that, while basic arithmetic operators and analytic functions on real numbers are Turing-computable, comparison of two real numbers is only semi-decidable [19].

Non-robustness issues are particularly serious in computational geometry in which combinatorial computations usually rely on numerical ones: small numerical inaccuracies turn into fatal inconsistencies in the combinatorial part of the computation. For example in the problem of Delaunay triangulation depicted in Figure 1, the effect of a small perturbation changing the point t to t' makes the previously legal edge vr illegal, while the previously illegal edge ut now becomes the legal edge ut'.

Computing with uncertain inputs is unavoidable in physical modelling [3], [15]. In applications such as robotics or solid modelling, actual geometric inputs are measurements of physical objects, and as such, they are inherently uncertain and can only be represented for example using intervals of numbers.

In our framework, geometric objects, i.e. subsets of $\mathbb{R}^d$, are captured by elements of the *solid domain* $\mathbf{S}\mathbb{R}^d$, which are called *partial solids* or *partial geometric objects* [5]. A geometric object is represented by a pair (I, E) of disjoint open sets, representing respectively the interior I and the exterior [4] E of the object. The information ordering is componentwise inclusion, i.e. $(I, E) \sqsubseteq (I', E')$ iff $I \subseteq I'$ and $E \subseteq E'$. The geometric object (I, E) is maximal in $\mathbf{S}\mathbb{R}^d$ iff $I = (E^c)^\circ$ and $E = (I^c)^\circ$, where X° and X^c denote respectively the interior and the complement of a set X. The collection of pairs of interiors of dyadic (or rational) polytopes forms a basis for $\mathbf{S}\mathbb{R}^d$. Any geometric object (I, E) can be obtained as the union of these basis elements.

Using the above model, we will show in this paper how to construct a partial Delaunay triangulation for a given set of N partial points. The partial Delaunay triangulation consists of partial edges. As the partial points tend to exact points, the partial Delaunay triangulation will converge to the Delaunay triangulation in the Hausdorff metric. A similar construction gives the partial Voronoi diagram of N partial points.

We will also examine the question of computability of the partial Delaunay triangulation and the partial Voronoi diagram. The standard notions of a computable element of a domain and a computable function between two domains provide us with the definition of a computable partial geometric object in $\mathbf{S}\mathbb{R}^d$, and a domain-theoretic computable function of type $f : (\mathbf{I}\mathbb{R}^d)^N \to \mathbf{S}\mathbb{R}^d$ or similar types, see [7].

Let X be $\mathbb{R}^d$ or a compact region such as $[-a, a]^d$. A computable function

$$\begin{aligned} f : \quad (\mathbf{I}X)^N \quad &\to \mathbf{S}X \\ (R_1, \ldots, R_N) &\mapsto (I(R_1, \ldots, R_N), E(R_1, \ldots, R_N)) \end{aligned}$$

is said to be effectively computable with respect to Hausdorff distance (volume or Lebesgue measure), if for any tuple $(R_1, \ldots, R_N)$ of recursive rectangles in $[-a, a]^d$ (i.e. rectangles with computable coordinates in $[-a, a]^d$), and any effective shrinking nested sequence of tuples of rational rectangles $(R_{1i}, \ldots, R_{Ni})$ (with $R_j = \cap_{i \geq 0} R_{ji}$), we can compute for any $m \in \mathbb{N}$, an integer n such that the Hausdorff distance between $\overline{I(R_1, \ldots, R_N)}$ and $\overline{I(R_{1n}, \ldots, R_{Nn})}$ (respectively the volume, or Lebesgue measure of the set-theoretic difference between $I(R_1, \ldots, R_N)$ and $I(R_{1n}, \ldots, R_{Nn})$) is bounded by 2^{-m} (and a similar relation on the exterior, $E(R_1, \ldots, R_N)$).

We will show that in this settings, the partial Delaunay triangulation and the partial Voronoi diagram are both computable and effectively computable

[4] The exterior of a set is the interior of its complement.

with respect to Hausdorff distance and Lebesgue measure.

For the full version of this paper, see [11].

2 Partial Voronoi Diagram

The problem of computing the partial Voronoi diagram of N partial points, i.e. N compact rectangles in the plane can be stated as follows. For a point $x \in \mathbb{R}^2$ and a compact rectangle $R \subset \mathbb{R}^2$, let $d_s(x, R) = \min\{|x - y| : y \in R\}$ and $d_l(x, R) = \max\{|x - y| : y \in R\}$ be, respectively, the shortest and longest distance from x to R. Now consider two rectangles R_i and R_j. The *interior of the partial Voronoi cell of R_i with respect to R_j* is given by $\mathcal{C}_{ij} = \{x \in \mathbb{R}^2 \mid d_l(x, R_i) < d_s(x, R_j)\}$. The *exterior of the partial Voronoi cell of R_i with respect to R_j* is given by $\mathcal{C}_{ji} = \{x \in \mathbb{R}^2 \mid d_l(x, R_j) < d_s(x, R_i)\}$. Note that interiors and exteriors are dual with respect to R_i and R_j: the interior of the partial Voronoi cell of R_j with respect to R_i is the exterior of the partial Voronoi cell of R_i with respect to R_j and vice versa.

The *interior of the partial Voronoi cell* of R_i is defined to be the set of points which are closer to any point in R_i than to any point in R_j ($j \neq i$). More precisely, $\mathrm{Int}(\mathcal{C}_i) = \{x \in \mathbb{R}^2 \mid \forall j \neq i;\ d_l(x, R_i) < d_s(x, R_j)\}$. The exterior of the partial Voronoi cell of R_i is defined to be the set $\mathrm{Ext}(\mathcal{C}_i) = \{x \in \mathbb{R}^2 \mid \exists j \neq i;\ d_l(x, R_j) < d_s(x, R_i)\}$. Thus, we have

$$\mathrm{Int}(\mathcal{C}_i) = \bigcap_{j \neq i} \mathcal{C}_{ij} \quad \text{and} \quad \mathrm{Ext}(\mathcal{C}_i) = \bigcup_{j \neq i} \mathcal{C}_{ji}.$$

Note that, even in the case that we only have line segments, the problem we address here is very different from the well-known problem referred to as "line segment Voronoi diagram" [1], which takes line segments as sites and considers the shortest distance to these segments. This is already illustrated in the simplest non-trivial case in Figure 2: there are only two rectangles R_1 and R_2 where R_1 is a degenerate rectangle containing only one point s and R_2 is a degenerate rectangle consisting of the vertical line segment uv, with $s \notin uv$. In this case, we have only two partial points, so $\mathcal{C}_1 = \mathcal{C}_{12}$ and $\mathcal{C}_2 = \mathcal{C}_{21}$.

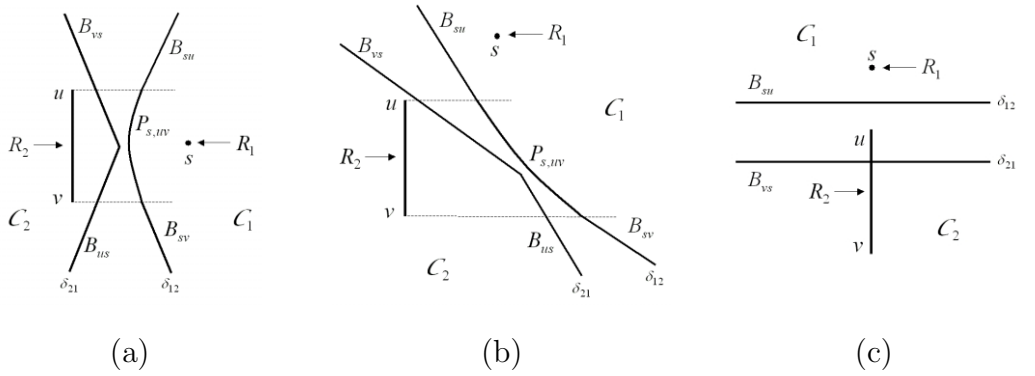

Fig. 2. Partial Voronoi diagram of one point and a line segment.

In Figures 2(a) and 2(b), where s, u and v are not collinear, the boundary of $\mathcal{C}_1$, namely $\delta_{12} = \{x \in \mathbb{R}^2 \mid d_l(x, R_1) = d_s(x, R_2)\}$, consists of the following three parts:

(i) the semi-infinite line B_{su}, part of the PB (Perpendicular Bisector) of su,

(ii) the segment $P_{s,uv}$ of the parabola with focus s and directrix passing through u and v,

(iii) the semi-infinite line B_{sv}, part of the PB of sv.

In the "line segment Voronoi diagram", δ_{12} is the boundary of the cell of R_1 and that of R_2, and provides the complete diagram. But in the new model we still need to find $\mathcal{C}_2$ whose boundary, $\delta_{21} = \{x \in \mathbb{R}^2 \mid d_l(x, R_2) = d_s(x, R_1)\}$, is different from δ_{12} and consists of the semi-infinite line B_{us}, part of the PB of us, and the semi-infinite line B_{vs}, part of the PB of vs. In Figure 2(c), that s, u and v are collinear, δ_{12} is the line B_{su} and δ_{21} is the line B_{vs}.

Note that even in this simple example the boundaries of the two regions do not coincide. In fact, the open region bounded by the two boundaries consists of points which are indeterminate, i.e. with the information available one cannot determine if they are in $\mathcal{C}_1$ or in $\mathcal{C}_2$. In terms of our model, $\mathcal{C}_1$ is the interior of the partial Voronoi cell of R_1 whereas $\mathcal{C}_2$ is the exterior of the partial Voronoi cell of R_1 (and vice versa for the partial Voronoi cell of R_2). If the input information is refined, i.e. if the line segment uv is shrunk, then some of the indeterminate points will fall in $\mathcal{C}_1$, i.e. the interior of R_1 expands, and some of the indeterminate points will fall in $\mathcal{C}_2$, i.e. the exterior of R_1 expands as well. In the limit when uv shrinks to a single point c, say, then the two boundaries tend to the PB of sc and we are in the classical case. Thus, in the presence of imprecise input, the set of indeterminate points will always have nonempty interior.

It is well known that, classically, the problem of the Voronoi diagram of a finite number of points in the plane can be reduced to computing the Delaunay triangulation of the set of points [2], [8]. We will see that the partial Voronoi diagram of a finite number of partial points, i.e. rectangles in the plane, can also be computed from a partial Delaunay triangulation of these partial points. Recall that three points of a given set of points in the plane form a partial Delaunay triangle if and only if their circumcircle does not contain any points of the set in its interior. The centre of the circumcircle is at the intersection point of the PB's.

We will see that in analogy with the classical case, the "partial Delaunay triangulation" of a finite set of partial points in the plane can be computed by determining the "partial circles" of the triples of partial points which do not contain any partial point in their interior. The "partial centre" of the partial circle passing through three partial points is computed by obtaining the intersection of the "partial PB's" of the three "partial edges".

3 Partial Perpendicular Bisector

The *partial PB* map is formally given by

$$\begin{aligned} \mathcal{B} : \mathbf{I}\mathbb{R}^2 \times \mathbf{I}\mathbb{R}^2 &\to \mathbf{S}\mathbb{R}^2 \\ (R_1, R_2) &\mapsto (\emptyset, \mathcal{C}_1 \cup \mathcal{C}_2), \end{aligned}$$

where $\mathcal{C}_1$ and $\mathcal{C}_2$ are the interiors of the partial Voronoi cells of R_1 and R_2 respectively, as defined in Section 2. Since the interior of the partial PB is always empty, we can identify $\mathcal{B}(R_1, R_2)$ with the closed set $(\mathcal{C}_1 \cup \mathcal{C}_2)^c$, where A^c denotes the complement of A. In the rest of the paper we therefore take:

$$\begin{aligned} &\mathcal{B}(R_1, R_2) = (\mathcal{C}_1 \cup \mathcal{C}_2)^c = \\ &\{z \in \mathbb{R}^2 \mid \exists x \in R_1,\ y \in R_2;\ |z - x| = |z - y|\}. \end{aligned} \tag{1}$$

What does $\mathcal{B}(R_1, R_2)$ look like in general? To see this, it is convenient to first obtain $\mathcal{C}_1$ for the case where R_1 is a degenerate rectangle consisting of a single point s and R_2 is a general rectangle. Clearly if $s \in R_2$ then $\mathcal{B}(R_1, R_2) = \mathbb{R}^2$. Otherwise, the boundary of $\mathcal{C}_1$ is depicted in Figure 3(a) for the case that s lies outside the closed vertical and horizontal strips induced by R_2. We see that the boundary δ_{12} of $\mathcal{C}_1$ is given by the line segment B_{sv}, part of the PB of sv, the two semi-infinite line segments B_{su} and B_{sr} and finally the two parabolic segments $P_{s,uv}$ and $P_{s,rv}$. Note that the two edges rt and tu are invisible from s and thus make no contribution to the boundary of $\mathcal{C}_1$. The boundary δ_{21} of $\mathcal{C}_2$ consists of one line segment B_{ts} and two semi-infinite line segments B_{us} and B_{rs}.

If s lies, say, on the horizontal strip of R_2 on the side of uv, then δ_{12} will be as in Figure 2(a). And δ_{21} will consist of two line segments B_{rs} and B_{ts}

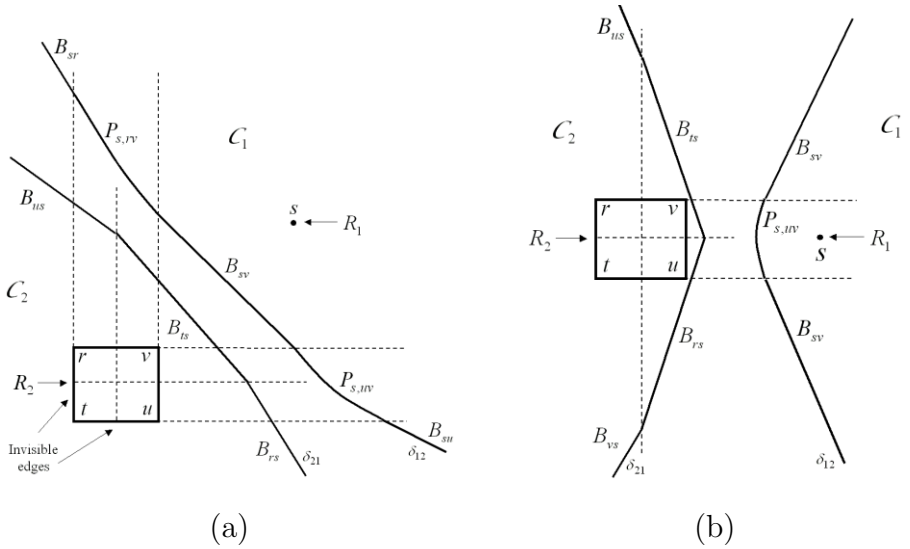

(a) (b)

Fig. 3. Partial Voronoi diagram of one point and a rectangle.

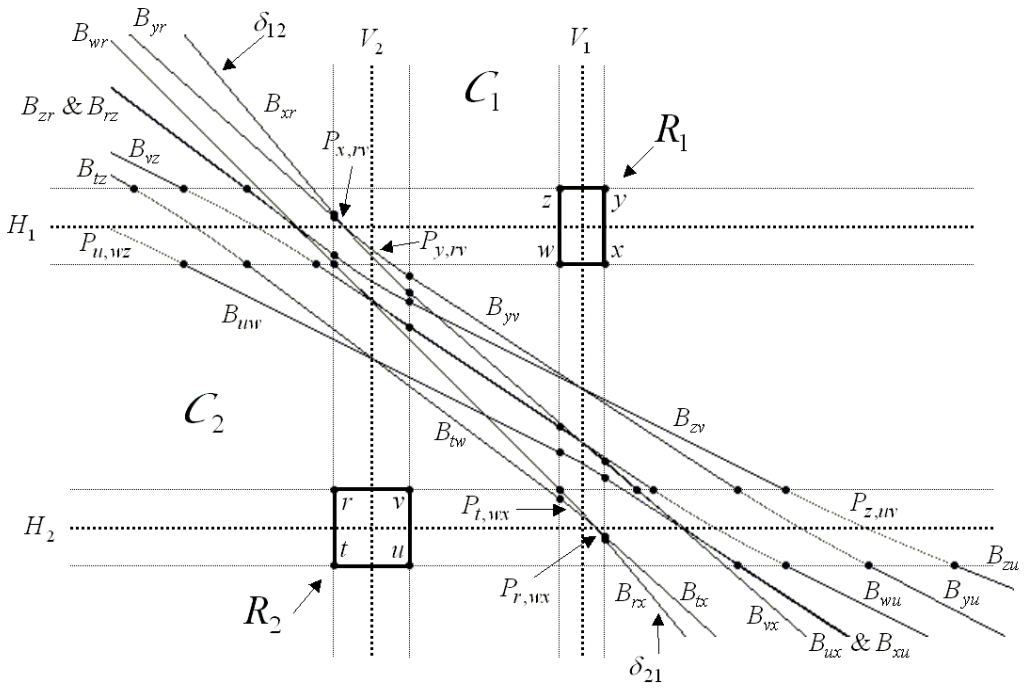

Fig. 4. Partial Voronoi diagram of two rectangles.

and two semi-infinite line segments B_{us} and B_{vs}, as depicted in Figure 3(b).

Proposition 3.1 *The partial Voronoi cell of a point with respect to a rectangle is the intersection of the partial Voronoi cells of the point and the visible edges of the rectangle.*

Proposition 3.2 *The partial Voronoi cell of a rectangle with respect to another rectangle is the intersection of the partial Voronoi cells of the vertices of the rectangle with respect to the other rectangle.*

Based on these results, we can determine the cells $\mathcal{C}_1$ and $\mathcal{C}_2$ of two non-intersecting but otherwise arbitrary compact rectangles R_1 (with vertices x, y, z, w) and R_2 (with vertices u, v, r, t) as shown in Figure 4, where we have assumed that the horizontal strips induced by R_1 and R_2 do not intersect, similarly for the vertical strips.

The interior $\mathcal{C}_{R_1R_2}$ of the partial Voronoi cell of R_1 is the intersection of the four interiors of the partial Voronoi cells $\mathcal{C}_{xR_2}$, $\mathcal{C}_{yR_2}$, $\mathcal{C}_{zR_2}$, and $\mathcal{C}_{wR_2}$. The boundaries of each of these open regions has, as we have just seen, three linear and two parabolic segments. The boundary δ_{12} of the intersection of the four interiors has seven linear and parabolic segments, which, as in Figure 4, are given by B_{xr}, $P_{x,rv}$, $P_{y,rv}$, B_{yv}, B_{zv}, $P_{z,uv}$ and B_{zu}. A similar boundary δ_{21} is obtained for the interior $\mathcal{C}_{R_2R_1}$ of the partial Voronoi cell of R_2.

Indeed, we can exactly identify which part of δ_{12} comes from the boundaries of $\mathcal{C}_{xR_2}$, $\mathcal{C}_{yR_2}$, $\mathcal{C}_{zR_2}$ and $\mathcal{C}_{wR_2}$. The horizontal line H_1 and the vertical line V_1 passing through the centre of R_1 divide the plane into four regions. In

each region, δ_{12} is part of the boundary of $\mathcal{C}_{sR_2}$, where s is the vertex in the diagonally opposite region. For example, in Figure 4, the semi-infinite line B_{xr} and a segment of $P_{x,rv}$ form the part of δ_{12}, which comes from the boundary of $\mathcal{C}_{xR_2}$. On the horizontal line H_1, δ_{12} changes from $P_{x,rv}$ to $P_{y,rv}$, which comes from the boundary of $\mathcal{C}_{yR_2}$ and continues with B_{yv}. On the vertical line V_1, δ_{12} changes from B_{yv} to B_{zv}, which comes from the boundary of $\mathcal{C}_{zR_2}$ and continues with $P_{z,uv}$ and the semi-infinite line B_{zu}.

Note that no part of the boundary of $\mathcal{C}_{wR_2}$ is used in δ_{12}, and no part of the boundary of $\mathcal{C}_{vR_1}$ is used in δ_{21}. This always happens when R_1 and R_2 do not intersect the horizontal and vertical strips of each other.

4 Partial Disc

We can now compute the partial disc whose boundary goes through three given partial points. For three non-collinear points $x, y, z \in \mathbb{R}^2$, let D_{xyz} be the unique closed disc whose boundary circle passes through x, y and z. Formally, we define the partial disc map by:

$$\begin{aligned} \mathcal{D}: \quad (\mathbf{I}\mathbb{R}^2)^3 &\to \mathbf{S}\mathbb{R}^2 \\ (R_1, R_2, R_3) &\mapsto (I, E), \end{aligned}$$

where $I = E = \emptyset$ if there exists a straight line which intersects R_1, R_2 and R_3, otherwise $I = (\bigcap\{D_{xyz} \mid x \in R_1,\ y \in R_2,\ z \in R_3\})^\circ$ and $E = (\bigcup\{D_{xyz} \mid x \in R_1,\ y \in R_2,\ z \in R_3\})^c$.

We will describe how to compute $I = I(R_1, R_2, R_3)$ and $E = E(R_1, R_2, R_3)$. We assume that R_1, R_2, R_3 satisfy the non-collinearity condition, namely that there exists no straight line which intersects all three rectangles. Then the intersection $\mathcal{O}(R_1, R_2, R_3) = \mathcal{B}(R_1, R_2) \cap \mathcal{B}(R_2, R_3) \cap \mathcal{B}(R_1, R_3)$ will in general be a compact set whose boundary consists of six vertices with six straight line and parabolic segments from δ_{12}, δ_{21}, δ_{13}, δ_{31}, δ_{23} and δ_{32} (Figure 5).

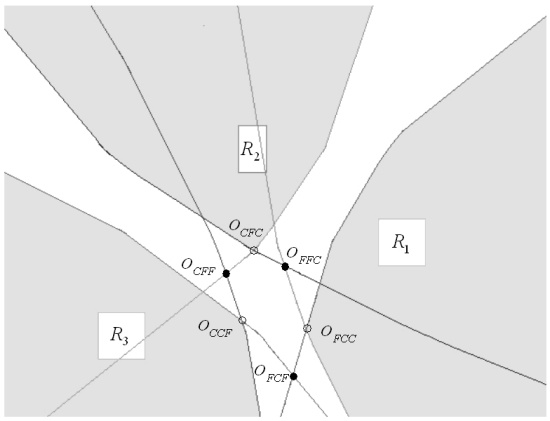

Fig. 5. Partial Voronoi diagram of three rectangles.

Proposition 4.1
$\mathcal{O}(R_1, R_2, R_3) = \{s \in \mathbb{R}^2 \mid \exists x \in R_1, y \in R_2, z \in R_3; |x-s| = |y-s| = |z-s|\}$.

Using the above proposition, we can say that $\mathcal{O}(R_1, R_2, R_3)$ is the locus of centres of circles which intersect R_1, R_2 and R_3; we call it the *partial centre* of the partial circumcircle of the three partial points. The vertices are given by

$$\begin{aligned} o_{CFC} &= \delta_{21} \cap \delta_{23}, & o_{FCF} &= \delta_{12} \cap \delta_{32}, \\ o_{CFF} &= \delta_{21} \cap \delta_{31}, & o_{CCF} &= \delta_{31} \cap \delta_{32}, \\ o_{FFC} &= \delta_{13} \cap \delta_{23}, & o_{FCC} &= \delta_{12} \cap \delta_{13}. \end{aligned}$$

Note that o_{CCF} is the centre of a circle with radius r_{CCF} which passes through (i) the point of R_1 closest to o_{CCF}, (ii) the point of R_2 closest to o_{CCF} and (iii) the point of R_3 furthest from o_{CCF}; hence the subscript in o_{CCF}. Similarly for the other vertices. If any one or more of the rectangles R_1, R_2 and R_3 are in fact singletons then some of these vertices coincide.

Proposition 4.2 *The set of vertices of the partial centre consists of the points o_{CCF}, o_{CFC}, o_{CFF}, o_{FCC}, o_{FCF} and o_{FFC}. If none of R_1, R_2 and R_3 is a singleton then the above six points are distinct. If R_1 is a singleton but not R_2 and R_3 then $o_{CFC} = o_{FFC}$ and $o_{CCF} = o_{FCF}$ and other points are distinct. If only R_1 and R_2 are singletons then we have two distinct points $o_{CFC} = o_{FCC} = o_{FFC}$ and $o_{CCF} = o_{CFF} = o_{FCF}$.*

Let $D(x, r)$ denote the closed disc with centre x and radius r. Consider the three discs $D_1 = D(o_{FCC}, r_{FCC})$, $D_2 = D(o_{CFC}, r_{CFC})$ and $D_3 = D(o_{CCF}, r_{CCF})$ on the one hand and the three discs $D'_1 = D(o_{CFF}, r_{CFF})$, $D'_2 = D(o_{FCF}, r_{FCF})$ and $D'_3 = D(o_{FFC}, r_{FFC})$ on the other hand.

Theorem 4.3 *The interior and the exterior of the partial disc $(I(R_1, R_2, R_3), E(R_1, R_2, R_3)) = \mathcal{D}(R_1, R_2, R_3)$ are given by:*

$$\begin{aligned} I(R_1, R_2, R_3) &= (D_1 \cap D_2 \cap D_3)^\circ \\ E(R_1, R_2, R_3) &= (D'_1 \cup D'_2 \cup D'_3)^c. \end{aligned}$$

In Figure 6, the boundaries of the discs D_1, D_2 and D_3 are depicted with dotted lines, those of D'_1, D'_2 and D'_3 with solid lines and the boundaries of the sets I and E with dashed lines. The closed region bounded between I and E, i.e. bounded between the two closed dashed curves, is called the *boundary of the partial disc*.

Using the above theorem, one can show:

Theorem 4.4 *The partial disc map $\mathcal{D}$ is Scott continuous (i.e. it preserves the partial order and the supremums of directed sets) and is effectively computable with respect to Hausdorff distance and Lebesgue measure.*

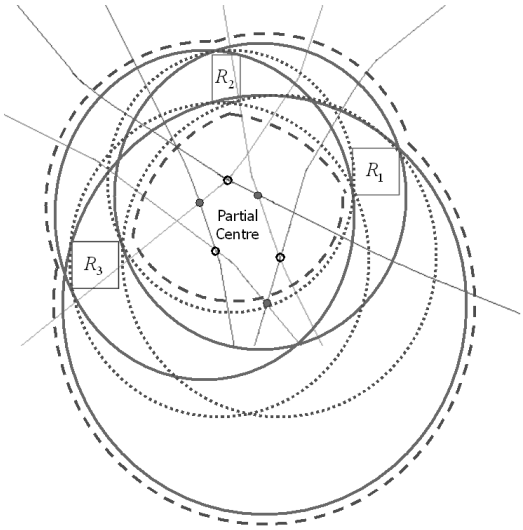

Fig. 6. The interior and exterior of a partial disc.

We now define the *containment* predicate

$$\mathrm{Con} : \mathbf{I}\mathbb{R}^2 \times (\mathbf{I}\mathbb{R}^2)^3 \to \{+,-\}_\perp$$

$$(R,(R_1,R_2,R_3)) \mapsto \begin{cases} + \text{ if } R \subset I(R_1,R_2,R_3) \\ - \text{ if } R \subset E(R_1,R_2,R_3) \\ \perp \text{ otherwise.} \end{cases}$$

Then it can be shown that Con is Scott continuous and is decidable on basis elements, which means that if the input $(R,(R_1,R_2,R_3))$ is a tuple of dyadic (or rational) rectangles, then we can decide in finite time if Con is true or false ($+$ or $-$) for this input. From this it will follow that Con is computable, i.e. given a computable tuple $(R,(R_1,R_2,R_3))$, then in *finite* time, i.e. by looking at only a finite number of the elements of the four sequences of basis elements approximating R and (R_1,R_2,R_3), we can verify that R is contained in the interior partial disc I or in the exterior partial disc E, i.e. containment in the interior and exterior of the partial circle is semi-decidable.

5 Partial Delaunay Triangulation

Suppose we are given N dyadic rectangles $R_1,\ldots,R_N$ in the plane. Given any i_1,i_2,i_3,i_4 with $1 \le i_1,i_2,i_3,i_4 \le N$, we can use the decidable predicate Con on dyadic or rational rectangles to determine if $R_{i_4} \subset I(R_{i_1},R_{i_2},R_{i_3})$ or if $R_{i_4} \subset E(R_{i_1},R_{i_2},R_{i_3})$.

Proposition 5.1 *Suppose four rectangles are given, any three of which satisfy the non-collinearity condition.*

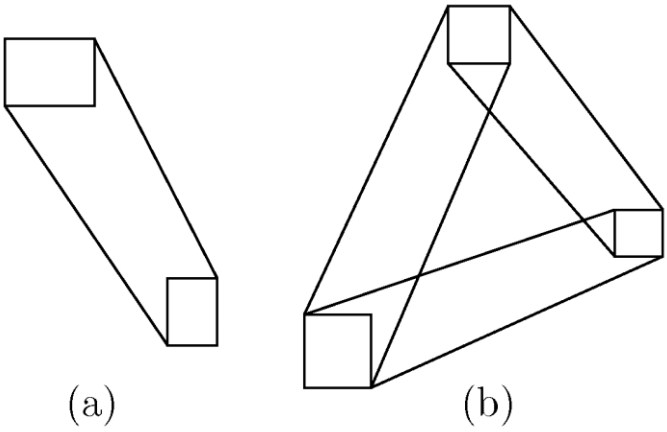

Fig. 7. Partial edge (a) and partial triangle (b).

(i) If one of the rectangles intersects the boundary of the partial disc of the other three rectangles, then any of the rectangles intersects the boundary of the partial disc of the other three rectangles.

(ii) If one of the rectangles is in the interior of the partial disc of the other three rectangles, then one of these three rectangles is in the exterior of the partial disc of the other three rectangles.

We define a partial edge between two partial points (closed rectangles) R_1 and R_2 to be the convex hull of R_1 and R_2, written $\mathrm{Ed}(R_1, R_2)$. We can also define a partial triangle to be the partial convex hull of three partial points (Figure 7).

Note that if the boundary of the partial disc of three rectangles intersects other rectangles, then the question of legality of the edges between the rectangles on the opposite side of the circle remains indeterminate at the present level of precision. Such cases occur in particular whenever a classical degenerate case is approximated, in which the circumcircle of a triangle contains a fourth point on its boundary. While some edges may remain indeterminate at a given stage of computation, the strength of the method lies in detecting those edges which are definitely legal or definitely illegal, so that the right choice can be made. This shows that our model also handles classical degenerate cases.

Therefore we define the partial Delaunay triangulation map as follows:

$$\begin{aligned}\mathcal{T}: \quad (\mathbf{I}\mathbb{R}^2)^N &\to \mathbf{S}\mathbb{R}^2\\ (R_1,\ldots,R_N) &\mapsto (\emptyset, (\bigcup\{\mathrm{Ed}(R_i,R_j) \mid \\ &\qquad \mathrm{Ed}(R_i,R_j) \text{ legal or indeterminate}\})^c).\end{aligned}$$

Theorem 5.2 *The partial Delaunay triangulation map $\mathcal{T}$ is Scott continuous and is effectively computable with respect to Hausdorff distance and Lebesgue measure.*

We finally discuss the question of computability of the partial Voronoi diagram. We define the partial Voronoi map on a list of N rectangles in the plane:

$$\mathcal{V} : (\mathbf{I}\mathbb{R}^2)^N \ \to \ (\mathbf{S}\mathbb{R}^2)^N,$$

with the ith component, $1 \leq i \leq N$, defined as

$$\mathcal{V}_i : (R_j)_{1\leq j\leq N} \ \mapsto \ (\mathrm{Int}(\mathcal{C}_i), \mathrm{Ext}(\mathcal{C}_i)),$$

where $(\mathrm{Int}(\mathcal{C}_i), \mathrm{Ext}(\mathcal{C}_i))$ was defined in Section 2. We now have:

Theorem 5.3 *The partial Voronoi map $\mathcal{V} : (\mathbf{I}\mathbb{R}^2)^N \ \to \ (\mathbf{S}\mathbb{R}^2)^N$ is Scott continuous and computable, and its restriction $\mathcal{V} : (\mathbf{I}[-a,a]^2)^N \ \to \ (\mathbf{S}[-a,a]^2)^N$ is effectively computable with respect to Hausdorff distance and Lebesgue measure.*

The concepts of partial points, partial edges, partial triangles, partial discs and the Con predicate are used in [12] to develop an algorithm to compute partial Delaunay triangulation, and thus the partial Voronoi diagram of N imprecise points.

6 Acknowledgment

We would like to thank John Howroyd for several useful discussions on this subject. This research has been funded by EPSRC.

References

[1] Aurenhammer, F. and R. Klein, *Voronoi diagrams*, in: J.-R. Sack and J. Urrutia, editors, *Handbook of computational geometry* (1999), pp. 201–290.

[2] de Berg, M., M. van Kreveld, M. Overmars and O. Schwarzkopf, "Computational geometry, algorithms and applications," Springer, 2000, 2nd edition.

[3] Desaulniers, H. and N. F. Stewart, *Robustness of numerical methods in geometric computation when problem data is uncertain*, Computer-Aided Design, special issue on uncertainties in geometrical design **25** (1993), pp. 539–545.

[4] Edalat, A. and A. Lieutier, *Domain theory and differential calculus*, submitted. Available from http://www.doc.ic.ac.uk/~ae.

[5] Edalat, A. and A. Lieutier, *Foundation of a computable solid modeling*, in: *Proceedings of the fifth symposium on Solid modeling and applications*, ACM Symposium on Solid Modeling and Applications, 1999, pp. 278–284.

[6] Edalat, A., A. Lieutier and E. Kashefi, *The convex hull in a new model of computation*, in: *Proc. 13th Canad. Conf. Comput. Geom.*, 2001, pp. 93–96.

[7] Edalat, A. and P. Sünderhauf, *A domain theoretic approach to computability on the real line*, Theoretical Computer Science **210** (1998), pp. 73–98.

[8] Fortune, S., *Voronoi diagrams and Delaunay triangulations*, in: D.-Z. Du and F. Hwang, editors, *Computing in Euclidean Geometry* (1992), pp. 193–233, lecture notes series on Comput.

[9] Gavrilova, M., H. Ratschek and J. G. Rokne, *Exact computation of Delaunay and power triangulations*, Reliable Computing **6** (2000), pp. 39–60.

[10] Karasick, M., D. Lieber and L. R. Nackman, *Efficient Delaunay triangulation using rational arithmetic*, ACM Transcations on Graphics **10** (1991), pp. 71–91.

[11] Khanban, A. A., A. Edalat and A. Lieutier, *Computability of partial Delaunay triangulation and Voronoi diagram*, http://www.doc.ic.ac.uk/~khanban.

[12] Khanban, A. A., A. Edalat and A. Lieutier, *Delaunay triangulation and Voronoi diagram with imprecise input data*, http://www.doc.ic.ac.uk/~khanban.

[13] Moore, R., *Methods and applications of interval analysis*, in: e. W. F. Ames, editor, *SIAM Studies in Applied Mathematics*, SIAM, 1979.

[14] Oishi, Y. and K. Sugihara, *Topology oriented divide-and-conquer algorithm for voroni diagrams*, Computer Vision,Graphics, and Image Processing: Graphical Models and Image Processing **57** (1995), pp. 303–314.

[15] Peters, T. J., D. R. Ferguson, N. F. Stewart and P. S. Fussell, *Algorithmic tolerances and semantics in data exchange*, ACM Conference on Computational Geometry (1997).

[16] Preparata, F. and M. Shamos, "Computational Geometry: an introduction," Springer Verlag, 1985.

[17] Sugihara, K. and M. Iri, *A robust topology-oriented incremental algorithm for voroni diagrams*, International Journal of Computational Geometry and Applications (1994), pp. 179–228.

[18] Sugihara, K., Y. Ooishi and T. Imai, *Topology-oriented approach to robustness and its application to several Voronoi-diagram algorithms*, in: *Proc. 2nd Canad. Conf. Comput. Geom.*, 1990, pp. 36–39.

[19] Weihrauch, K., "Computability," EATCS Monographs on Theoretical Computer Science **9**, Springer-Verlag, 1987.